Sensors and Materials, Vol. 9, No. 8 (1997) 521–540
MYU Tokyo

S & M 0309

Excitation and Detection of Silicon-Based Micromechanical Resonators

Harrie A. C. Tilmans† and Siebe Bouwstra*

Katholieke Universiteit Leuven, Departement Elektrotechniek-ESAT,
Kardinaal Mercierlaan 94, B-3001 Heverlee, Belgium
*Technical University of Denmark, Mikroelektronik Centret, Building 345 East,
DK-2800 Lyngby, Denmark

Key words: resonator, transduction, one-port, two-port, excitation, detection, equivalent circuit, micromechanics, modal analysis

Mechanical resonators operate in the mechanical domain, but the exchange of information takes place in the electrical domain. A crucial design issue of a mechanical resonator therefore concerns the elements that are necessary for electromechanical signal conversion. A mechanical resonator is brought into vibrational motion by an excitation element, and subsequently, the motion is sensed by a detection element. In this paper we review a wide range of physical transduction mechanisms that can be exploited for electromechanical signal conversion. Furthermore, the possible electrical configurations, termed one- and two-port resonators, and the relevance of the spatial placement of the transducer elements with respect to the position of the vibrating member, are discussed. Finally, a more quantitative analysis and equivalent circuit representations are presented. It is concluded that the paper provides a guide for selecting the most suitable mechanism and appropriate electrical and mechanical configurations for a specific application.

1. Introduction

Recent work on micromechanical *silicon-based* resonators has indicated their great potential as strain,[1–19] shape[20] and mass[21] sensing elements in mechanical sensors, as vibration sensors,[22] as ultrasonic proximity sensors,[23] as (tuned) electromechanical filters,[24–26] as driving elements of a micromotor,[27] as the shutter element in a noncontacting

†Present address: CP Clare Corporation, Bampslaan 17, B-3500 Hasselt, Belgium

voltage meter[28] and as (tuned) frequency references in electronic systems.[29] As resonant strain sensing elements they have been demonstrated in, for example, pressure sensors,[4–6,11,12,18] force sensors,[9,10,14,15,17] flow sensors[8] and accelerometers.[7,19]

One of the crucial design issues of the resonator concerns the elements that are necessary for electromechanical signal conversion. The mechanical resonator is brought into vibrational motion by means of an *excitation element*, and the motion is sensed using a *detection element*. A number of physical effects, such as the piezoelectric effect, can be exploited to accomplish this. Emphasis is put here on the use of silicon-based materials as the bulk material as opposed to quartz or gallium-arsenide-based resonators. The latter make direct use of the piezoelectric properties of the bulk material for excitation and detection and will not be considered in this paper. It goes without saying that the discussion below applies to any other nonpiezoelectric material besides silicon. In addition, from an electrical point of view and depending on the number of elements used, several driving configurations, designated as *one-*, *two-* or *N-port* resonators, are possible. Mechanical configurations vary from *integrated* or *on-chip* excitation/detection to *external* or *off-chip* excitation/detection and depend on the position of the elements with respect to that of the vibrating member. The purpose of this paper is to review and summarize the foregoing issues in a qualitative and also to some extent a quantitative way. This approach allows a comparison of the available options and sets this paper apart from other recently published reviews.[13,30–33] Verification of the presented material using actual resonators is considered to be beyond the scope of this paper. However, a large number of references to the existing literature will be given in order to back up the theory.

2. Physical Transduction Mechanisms

Excitation and detection of vibrational motion require signal conversion from the electrical to the mechanical domain, and vice versa, respectively. Whereas in quartz-based resonators direct use is made of the piezoelectric properties of quartz for electromechanical signal conversion, in silicon-based resonators special provisions have to be made. Figure 1 shows the basic configurations, employing a number of different physical transduction mechanisms that can be used for this purpose. Flexural-type resonators are used for illustrative purposes, but the results are easily interpreted for other types of resonators, *e.g.*, torsional or laterally driven resonators. Unless explicitly indicated no distinction is made between excitation and detection. Furthermore, a bias (either internal or external) is essential to ensure electromechanical transduction and/or to attain small signal *linear* interactions between the electrical and mechanical variables.

Figure 1(a) illustrates the *electrostatic* transduction.[3,10,12,15,16,20,21,24,25,34–38] Here, the driving load q is the Coulomb attractive force between the two charged plates or electrodes of a capacitor. One electrode is formed by (a part of) the beam and the other by a (stationary) surface located close to the beam. The detection is *capacitive*, based on the fact that a variation of the distance between the plates results in capacitance fluctuations, inducing either an a.c. current in case of a d.c. voltage bias, or an a.c. voltage in case of a given bias charge.

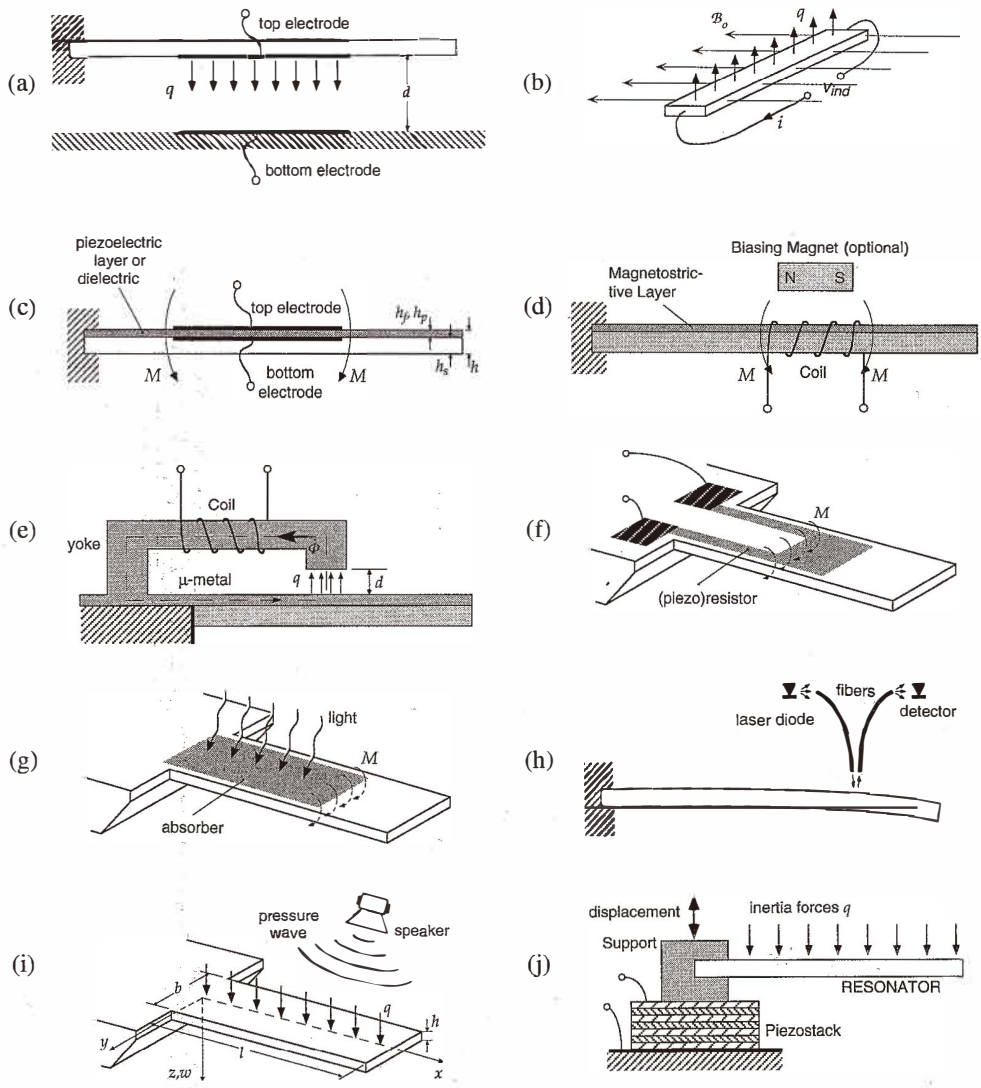

Fig. 1. Schematic representation of transduction mechanisms used for excitation and detection of the vibrational motion of (micro) mechanical resonators. The driving forces per unit length and the driving moments are indicated by q and M, respectively. The positioning of the elements is arbitrarily chosen. (a) electrostatic excitation/detection, (b) electrodynamic excitation/detection, (c) piezoelectric and dielectric excitation/detection, (d) magnetostrictive excitation/detection; either a permanent magnet (drawn) or an electromagnet may be used for biasing purposes, (e) electromagnetic excitation/detection, (f) electrothermal excitation/piezoresistive detection, (g) optothermal excitation, (h) optical displacement detection, (i) acoustic excitation, (j) "shaker" excitation.

For the *electrodynamic* principle,[6,14,39] the beam is placed in an external bias magnetic field with induction B_0. The Lorentz force which acts on the applied current $i(t)$ provides the driving force q. Due to the motion of the beam, the flux linkage of the current loop changes, thereby inducing a voltage v_{ind} which provides the detection signal.

Piezoelectric excitation and *detection*[2,4,9,17,19,40] (Fig. 1(c)) are based on the inverse piezoelectric effect and the direct piezoelectric effect, respectively.[41,42] A piezoelectric material provides its own *internal* bias, due either to the absence of a center of symmetry in single crystal materials (*e.g.*, zinc oxide (ZnO)),[41–45] or to a permanent polarization in the case of ferroelectric materials (*e.g.*, ferroelectrics of the lead zirconate titanate (PZT) family).[41,42,46,47] The inverse piezoelectric effect is manifested as a mechanical deformation in the material subjected to an electric field. If the piezoelement is fixed on top of the beam, a bending moment M will be induced which is used to excite the beam. Conversely, through the direct piezoelectric effect, a mechanical deformation will affect the electric charge distribution, which can be detected as electric current or voltage at the terminals.

Dielectric excitation[48] (Fig. 1(c)) is based on the lateral deformation of a dielectric thin film, sandwiched between a top and a bottom electrode, due to an electrostatic force arising if a voltage is applied across the electrodes. The lateral deformation will cause bending moments M that are used to drive the structure. The detection is *capacitive*, based on the change in the capacitance of a dielectric capacitor if the dielectric is deformed.

Magnetostrictive transduction (Fig. 1(d)) is based on the change in dimensions of ferromagnetic materials when exposed to a magnetic field. The term also applies to the inverse effect, that is, there is a change in magnetization or the generation of a magnetic field when the material is externally stressed. A true piezomagnetic effect comparable to the true piezoelectric effect due to the absence of a center of symmetry in single crystals has not been demonstrated yet. However, magnetostriction in the presence of polarization, due either to a permanent magnetic polarization present in ferromagnetic materials, or to an externally applied bias magnetic field, is phenomenologically equivalent to piezomagnetism.[41,49] Promising thin film magnetostrictive layers consist of alloys of iron with rare-earth materials such as terbium (Tb), dysprosium (Dy) and samarium (Sm), *e.g.*, terfenol-D alloys.[49–51]

The *electromagnetic transducer* (Fig. 1(e)) forms the dual analogue of the electrostatic transducer. The structure consists of a yoke, a resonating beam and a driving coil with an excitation winding of N turns. A d.c. current in the coil induces a bias magnetic flux in the yoke and the gap. The yoke and an upper layer of the beam (or the entire beam) consist of a highly permeable material, i.e., $\mu_r \rightarrow \infty$, and are separated by a gap, usually filled with air or a vacuum. Together they form a magnetic circuit through which a magnetic flux Φ flows. The total reluctance, defined as the ratio of the magnetomotive force to the flux passing through the magnetic circuit, is approximately equal to the reluctance of the air gap. Hence, the magnitude of the flux is controlled by the gap spacing. The distributed magnetic force induced in the gap provides the driving force q. The resulting motion of the resonator leads to a change in the reluctance, and thus to a change in the flux passing through the circuit. Based on Faraday's law of electromagnetic induction, this induces an a.c. detection voltage across the electric terminals of the coil.[52,53]

Electrothermal excitation[5,7,8,10,23,54–60] (Fig. 1(f)) is based on thermal expansion due to

temperature elevation as a result of heat generation by an electrical current in a resistor. If the resistor is located in the upper fibers of the beam a thermal wave propagating and attenuating in the thickness direction results. This in turn creates a bending moment M, which is used to excite the beam. To avoid frequency doubling, a d.c. bias voltage or current is superimposed onto the a.c. drive signal.

The electromechanical transducers described in Figs. 1(a)–1(e) are all based on reversible mechanisms. In other words, electric energy can be converted into mechanical energy, and vice versa, which allows both excitation and detection of the vibrational motion. Due to the irreversible conversion of electric energy into heat in the thermal transducer, the detection must be accomplished through other means. In Fig. 1(f), beam deformation is detected as a modulation of the resistance due to the *piezoresistive effect*.[5,8,10,12,22,23,25,54,55,58,59] In this way, the detection is fully compatible with the excitation, i.e., the same type of resistor can be used for both excitation and detection of the vibration.[5,8,10,23,54,55,58,59]

The basic principle of *optothermal excitation* (Fig. 1(g)) is the same as that of electrothermal excitation. The difference is the heat source, which is formed by the absorption of light by bare silicon or an absorbing layer, *e.g.*, aluminum.[57,61–68] Several techniques are used for *optical detection*, such as intensity modulation due to interruptions of the light beam by the resonator,[60,69,70] use of an optical proximity or displacement sensor as shown in Fig. 1(h),[4,56,61,70,71] or interferometric techniques.[32,62–64,68,72–74]

Two external excitation methods are *acoustic excitation* (Fig. 1(i)) and the "*shaker*" method (Fig. 1(j)). In the former, the ambient pressure provides the necessary bias, and pressure (sound) waves or fluctuations cause a distributed driving force.[23] In the latter, a piezostack or vibration table for instance, causes (harmonic) displacements of the entire structure, including the support and the resonator. The resulting inertia forces acting on the resonator provide the driving load q.[11,22,73] In theory, acoustic detection, *e.g.*, sensing the sound waves transmitted by the vibrating structure using a microphone,[23,56] and detection via the reverse piezoelectric effect in the material of the piezostack are possible, but in practice the effects are often too small to be of any practical use. Thus, for the methods shown in Figs. 1(i) and 1(j), detection must be accomplished through different techniques, *e.g.*, optical interrogation.[11]

Besides the basic transduction mechanisms depicted in Fig. 1, other more complex methods exist, for instance the field-effect modulation of the channel conductance of a MOSFET which can be used for detection purposes,[24] or the shape memory effect of certain alloys (SMA's),[75] which can be used for excitation purposes. Also note that a combination of mechanisms can be used within a single resonator, *e.g.*, see refs. 10, 12, 24, 25, 58, 60, 76. The choice of a particular mechanism is based on a number of considerations including the complexity and availability of a particular fabrication technology, IC compatibility, power consumption and the impact the element has on the resonator characteristics, for instance aging and drift properties and the temperature dependence of the resonant frequency. None of the aforementioned mechanisms are considered to be the ideal method for excitation and detection. Table 1 summarizes a number of characteristics of the different mechanisms, and should assist in deciding on a suitable mechanism.

Table 1
Comparison of some characteristics of the transducer mechanisms shown in Fig. 1.

Transduction Mechanism	Load type	Bias	On-chip Power Consumption	Complexity[3] of technology	IC compatible?	Influence on resonator characteristics
Electrostatic	*force*	external *E*-field[1]	low	+/–	yes	medium
Electrodynamic	*force*	external *B*-field	medium	+/–	yes	small
Dielectric	*moment*	external *E*-field[1]	low	+/–	yes	large
Piezoelectric	*moment*	internal *E*-field	low	+	no	large
Magnetostrictive	*moment*	ext. or int. *B*-field[2]	medium	++	no	large
Electromagnetic	*force*	external *B*-field	medium	++	no	medium
Electrothermal exc.	*moment*	temp. elevation	high	–	yes	medium[5]
Piezoresistive det.	–	external *E*-field	high	–	yes	medium[5]
Optothermal exc.	*moment*	temp. elevation	high	++[4]	yes/no	small[5]
Optical detection	–	–	low	++[4]	yes/no	small[5]
Acoustic exc.	*force*	base pressure	low	– –	yes	small
Shaker exc.	*displacement*	–	low	– –	yes	small

1) Usually by applying a d.c. voltage; built-in bias charge is also possible.
2) Depending on the magnetostrictive material used, e.g., ferromagnetic materials provide their own *internal* bias.
3) The symbols indicate: bare structures (– –), not complex (–), moderately complex (+/–), complex (+), very complex because of mounting of discrete components (++).
4) Resonator structure itself can be rather simple; complexity is due to the necessary optical components/setup.
5) It is noted that, *e.g.*, for bridge resonators, a static temperature elevation induces an axial stress that may significantly affect the resonant frequency.[8,77]

3. External versus Integrated Transduction Elements

Since the applied materials and the mechanical configuration of the excitation/detection elements are usually not optimized for mechanical properties, but instead for electromechanical transduction, the elements can have a detrimental influence on the resonator characteristics, such as the resonant frequency and aging and drift properties. Moreover, dissipation of heat within the elements can lead to thermal stresses that may cause undesirable and unreproducible shifts of the resonant frequency.[8,65,77,78] In this context it is pointed out that the resonator characteristics are primarily a function of the structure itself (geometry, elastic material properties, residual stress, interfacial contact between different layers of materials). However, the resonator characteristics can, to some extent, also be determined by the *spatial placement* of the elements with respect to the position of the vibrating member. A wide variety of possible placements exists, as is clearly illustrated in Fig. 1. Generally speaking, the elements can be placed *external* to the resonator, or, they can be *integrated* with the resonator. Examples of external elements are the speaker in Fig. 1(i), the piezostack in Fig. 1(j), the light source in Fig. 1(g) and the optical detection unit in Fig. 1(h). The remaining configurations of Fig. 1 are examples of integrated mechanisms.

It is understandable that the influence of the elements is less pronounced on the external mechanisms. For obvious reasons, the external drive is not suited for applications in practical devices. Instead they prove to be very useful during the research stage of a prototype resonator for obtaining a better insight into the latters' behavior. Also, since in the case of the external drive, the resonator can only be of a simple geometry and can be composed of a single material only, this method is particularly useful for the extraction of material parameters, such as Young's modulus and residual stress.[37,79,80]

Integrated mechanisms are further divided into mechanisms whereby the driving load is due to *distributed body forces* acting on modified parts of the resonator, or to *internal deformations* within the resonator itself. Gradients in the internal deformations lead to equivalent bending moments M exerted on the resonator. Mechanisms belonging to this category are dielectric, piezoelectric, magnetostrictive, and the electro- and optothermal drives. Distributed body forces act directly on the distribution of matter, *e.g.*, charged particles that are placed in an electric field are subjected to an electrostatic force, which lead to transverse driving forces q. Examples belonging to this class of mechanisms include the electrostatic, electrodynamic and electromagnetic drives. For these mechanisms, necessary adaptations to be made to the resonator are generally less radical compared to the mechanisms that rely on internal deformations. For instance, in general the latter require a multilayered structure (*e.g.* as in Fig. 1(c)), whereas this is not necessary for "body force mechanisms" (*e.g.*, as in Fig. 1(a)). As a result, the influences on the resonator characteristics of transduction elements based on body forces are smaller for this class of mechanisms.

By moving the integrated excitation/detection elements further towards the support or the base of the resonator, some degrading influences of the elements on the resonator characteristics can be strongly reduced. An example of such a configuration is shown in Fig. 2. Thermal and/or electrostatic drive elements that are integrated in the base of a resonator cause both translational ($w(0)$) and rotational displacements ($\phi(0)$) of the cantile-

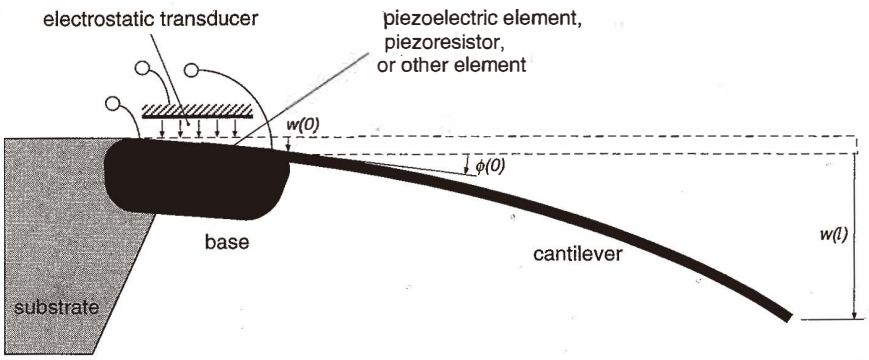

Fig. 2. Example of base (or support) excitation. The cantilever resonator is excited at the base using a piezoelectric, electrothermal or electrostatic excitation transducer element. The motion is also sensed at the base, *e.g.*, using a piezoelectric, piezoresistive or electrostatic transducer element.

ver's fixed end. This in turn induces inertia forces[81,82] that form the actual driving force. Damping forces are also induced, but these are generally negligible.[82] Conversely, resonator motion causes displacements/deformations of the base which are subsequently picked up by the transduction elements. Configurations of this kind are collectively called *base or support excitation/detection*.[81–83] For these configurations, it is actually the base of the resonator that is brought into a vibrational motion, or on which the deformation is measured. In a true sense, however, the base forms an integral part of the resonator. In order to detect any excitation and/or detection, the base should have finite stiffness; on the other hand, a too compliant base can adversely affect the resonator characteristics. The challenge lies therefore in finding a compromise between sufficient excitation/detection and a minimal effect of the base on the resonator characteristics. For a more detailed discussion and other examples of base drive, the reader is referred to the literature.[82,83]

4. Electrical Configuration

In general, two approaches can be used for the excitation and detection of the vibrational motion of a mechanical resonator. One approach uses a single transducer element or single electric terminal pair for both excitation and detection and as such defines an electrical one-port network.[16,34,37,38,55,84] The other approach uses two physically separate transducer elements. This results in two electric terminal pairs or ports, one used for excitation and the other for detection of the vibration.[2–10,12,14,17–26] Here, an electrical signal or electric energy enters the excitation terminals, is acted upon by the network, i.e., the resonator, and leaves via the detection terminals. The above has led to the designation *one-port resonators* and *two-port resonators*. The basic configurations are schematically shown in Fig. 3.

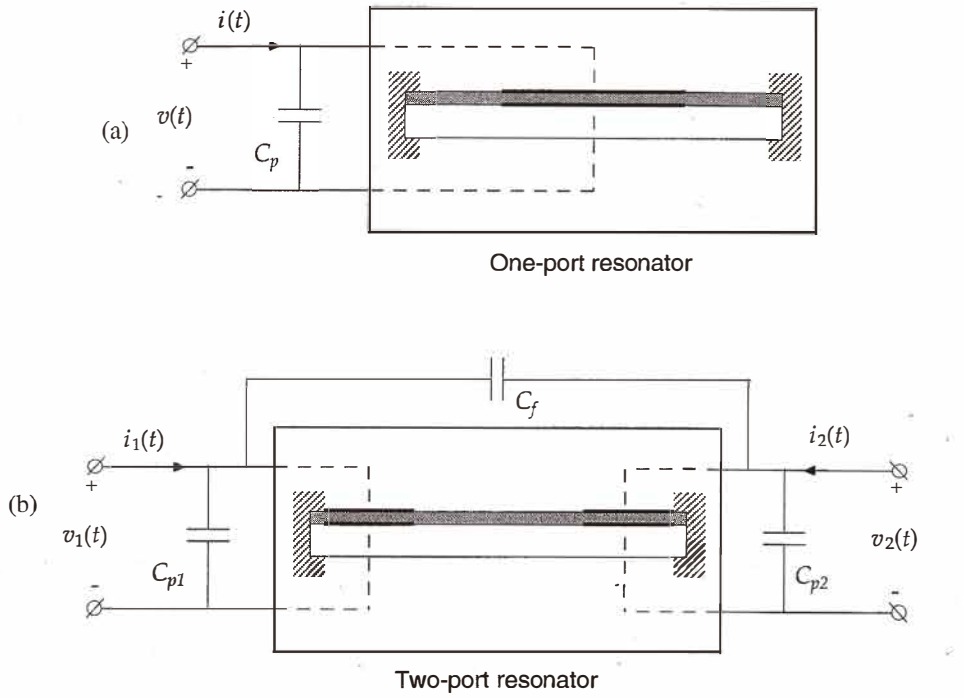

Fig. 3. Electrical resonator configurations illustrated for a piezoelectrically driven resonator. (a) One-port resonator: The resonator characteristics can be derived from the measured impedance (v/i) or the admittance (i/v) at the electric port; C_p denotes a parasitic parallel capacitor. (b) Two-port resonator: One of the ports is used for excitation while the other is used for the detection of vibration. Any of the four possible transfer functions (i_2/v_1, i_2/i_1, v_2/v_1, v_2/i_1) can be used to extract the resonator characteristics; C_{p1} and C_{p2} denote parasitic capacitors connected parallel to the port terminals, and C_f denotes a feedthrough capacitor connecting the two ports.

In the frequency domain, a linear electric one-port network can be characterized either by its *impedance* $Z(jw) \equiv v/i$ or by its *admittance* $Y(jw) \equiv i/v$, where v and i denote the complex amplitudes of the sinusoidal voltage across the port terminals and the total current flowing into (or out of) the port, respectively (see Fig. 3(a)). As a rule, the impedance formulation is utilized if the resonator is driven from a current source, taking the voltage as the response: $v = Z(jw)i$. In other words, the current is taken as the imposed variable and the voltage as the deduced variable. Conversely, if the voltage is taken as the imposed variable with the current as the deduced variable, the admittance formulation is preferred: $i = Y(jw)v$. The question as to whether the impedance or the admittance is best suited as the descriptive function largely depends on the nature of the transduction mechanism used for excitation/detection.[53]

A two-port network is characterized by the two voltage-current pairs of the electric

ports: $\{v_1,i_1\}$ and $\{v_2,i_2\}$ (Fig. 3(b)). As known from standard network theory, the relation between the electric port variables can be expressed in terms of either *admittance*, *impedance* or *hybrid* parameters. For instance, in full matrix notation the admittance formulation is as follows:

$$\begin{Bmatrix} i_1 \\ i_2 \end{Bmatrix} = \begin{bmatrix} Y_{11} & Y_{12} \\ Y_{21} & Y_{22} \end{bmatrix} \begin{Bmatrix} v_1 \\ v_2 \end{Bmatrix}, \tag{1}$$

where the admittance parameters, i.e., the coefficients of the admittance matrix, are defined as: $Y_{11} \equiv i_1/v_1\,|_{v_2=0}$, $Y_{12} \equiv i_1/v_2\,|_{v_1=0}$, $Y_{21} \equiv i_2/v_1\,|_{v_2=0}$ and $Y_{22} \equiv i_2/v_2\,|_{v_1=0}$. Similar relations exist for the remaining two parameter sets as explained in any standard textbook on electric network theory (*e.g.*, see ref. 85).

In both approaches, spurious responses can obscure the mechanical resonance. For the two-port configuration, this is caused by electrical feedthrough from the excitation port to the detection port, for instance due to the feedthrough capacitance C_f as shown in Fig. 3(b).[21,40,58] For the one-port configuration electrical feedthrough (by definition) does not exist, since there is only one port. However, here a parasitic load, such as the parasitic parallel capacitance C_p in Fig. 3(a), has a similar degrading effect.[37] The choice of a specific approach depends on the choice of transduction mechanism, on the complexity of the layout and fabrication process, on the electronic circuitry used for the sustaining oscillator, and on the question of whether the problem of spurious response as mentioned above can adequately be solved or not. In this context it is pointed out that a one-port resonator always suffers from parasitic loads. For instance, for an electrostatically driven one-port resonator the static capacitance is always present and as such already has a degrading effect. A two-port resonator on the other hand can (theoretically) be designed without any electric feedthrough. For instance, consider an electrostatically driven two-port resonator whereby the voltage v_1 is taken as the driving signal and the current i_2 as the detection signal. In the absence of any feedthrough loads and if the current i_2 is measured through a short (or low impedance) circuit ($v_2 = 0$), thus shorting out the static capacitance of the detection port, the transadmittance i_2/v_1 is equal to Y_{21}, which gives an ideal transfer behavior.[86,87]

For both one- and two-port resonators, suppression of the influence of parasitic loads can be accomplished through specific compensation techniques that are based on differential measurements.[53,87,88] Another method used for two-port resonators employs shielding between the excitation and detection ports[58] in order to reduce the feedthrough capacitance.

Among the mechanisms indicated in Fig. 1, a special class is formed by the optical interrogation methods. Since light is easily confined to a given space, optical feedthrough or coupling between the excitation port, *e.g.*, electro- or optothermal, and the optical detection port can be kept negligibly small. In general, feedthrough and parasitic loads are not confined to the electrical or optical domain, but can also exist in for instance the thermal or mechanical domain. In a trivial design, however, these effects are easily avoided.

5. Quantative Aspects and Equivalent Networks

The mathematical formulations given below are restricted to flexural resonators, consisting of initially flat, prismatic, homogeneous, wide (i.e., $b > 5h$) cantilever (zero axial force) beams ($l \gg b$) with a rectangular cross section as depicted in Fig. 1(i). Small vibrational motions $w(x,t)$ about the equilibrium position are governed by the following linearized equation of motion:[53]

$$\hat{E}I\frac{\partial^4 w(x,t)}{\partial x^4} + c\frac{\partial w(x,t)}{\partial t} + \rho bh\frac{\partial^2 w(x,t)}{\partial t^2} = q(x,t) - \frac{\partial^2 M(x,t)}{\partial x^2}, \tag{2}$$

where $\hat{E} = E/(1-\nu^2)$ is the plate modulus, and E and ν are Young's modulus and Poisson's ratio of the beam material, respectively, ρ denotes the specific mass of the beam material, b and h denote the width and thickness of the beam, respectively, I ($= bh^3/12$) is the second moment of inertia of the beam cross section, c is the viscous drag parameter, and $q(x,t)$ and $M(x,t)$ denote the externally applied driving force per unit length and driving moment, respectively. The natural frequencies ω_n are found by solving the homogeneous part of eq. (2).[13] At the fundamental frequency and ignoring the effects of electromechanical coupling,[53] this results in: $\omega_1 = \sqrt{K_1/M_1}$, where $K_1 = 1.03\hat{E}b(h/l)^3$ and $M_1 = \rho bhl$, representing the modal (or generalized) stiffness and mass, respectively. Hereby, the mode shapes are normalized such that the modal mass equals the total mass of the beam.

To obtain a description of the *electromechanical behavior* of the resonator, eq. (2) is solved in conjunction with the constitutive equations of the transducer elements. The latter relate the electric port variables such as voltage and charge to the mechanical port variables, *e.g.*, force and displacement.[32,52,53,86,87] The resulting expressions of the electric transfer functions as introduced in the previous section are subsequently used as a starting point for synthesizing the equivalent electric circuit diagrams. It is beyond the scope of this paper to go into further detail at this point, but it can be shown that the main parts (see also the discussion at the end of this Section) of the different transducers of Fig. 1 can conveniently be modelled by the equivalent electric networks shown in Fig. 4.[53,86,87] The networks are applicable within a frequency regime in the vicinity of the fundamental resonance. The influence of higher order modes is accounted for by adding parallel branches to the mechanical site, one for every mode of vibration.[53,87] The mechanical port associated with the fundamental mode is conveniently defined by the following *generalized* load-velocity pair $\{P_1(t),\xi_1(t)\}$.[86,87] The generalized port variables are introduced if the equation of motion is solved using the theory of *modal analysis*.[89] Hereby, the beam deflection is regarded as a superposition of system eigenfunctions or mode shapes $\phi_n(x)$ multiplied by the corresponding time-dependent generalized coordinates $\xi_n(t)$: $w(x,t) = \sum\xi_n(t)\phi_n(x)$.[81,89] Generalized loads associated with the fundamental mode can be obtained from the true physical load as the dot product of the latter and $\phi_1(x)$,[89] *e.g.*, for the external driving loads of eq. (2) it follows that $P_{d1}=\int[q(x) - \partial^2 M(x)/\partial x^2]\phi_1(x)dx$. For instance, for a point force F_o applied at $x = x_1$, this amounts to $F_o\phi_1(x_1)$; for a point moment M_o applied at $x = x_1$, the generalized force equals $M_o\phi_1'(x_1)$; and for a uniformly distributed force per

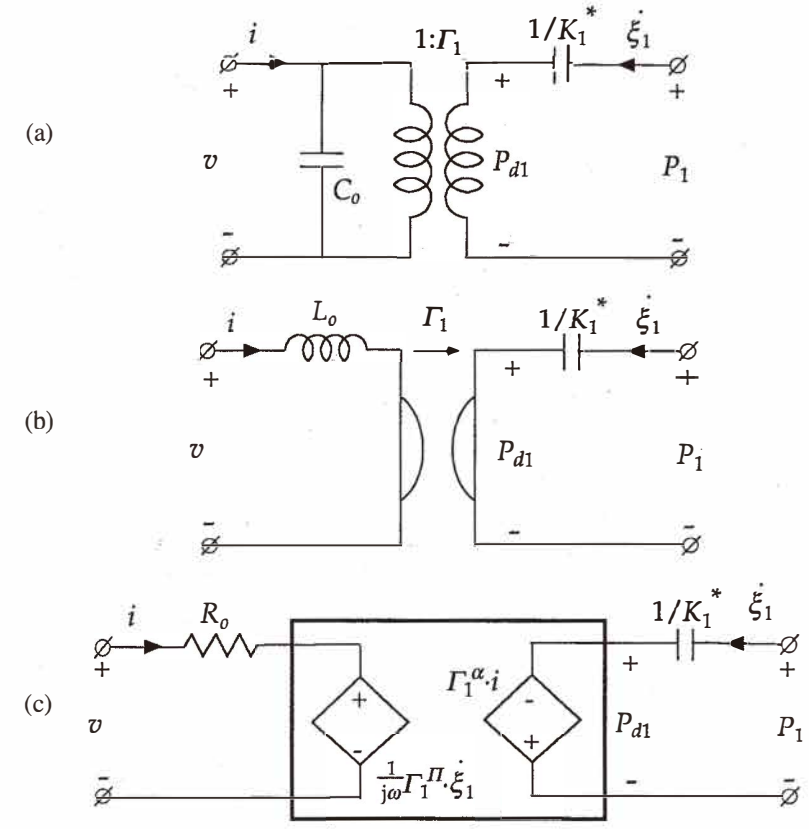

Fig. 4. Equivalent electric networks of a number of electromechanical transducer elements applicable in the vicinity of the fundamental mode. The meaning of the symbols is explained in Appendix I (see also Table 2). (a) Equivalent network of the electrostatic, piezoelectric and dielectric transducers. (b) Equivalent network of the electrodynamic, electromagnetic and magnetostrictive transducers. (c) Equivalent network representing electrothermal excitation and piezoresistive detection.

unit length $q(x) = q_o$, one obtains $q_o\int\phi_1(x)dx = 0.783q_ol$. The electromechanical signal conversion is modelled either by a transformer with converts ratio Γ_1 in units of N/V (Fig. 4(a)) or N/A (Fig. 4(b)), or by current-controlled voltage sources with proportionality constants Γ_1^α (in N/A) and Γ_1^π (in V/m), representing electrothermal excitation and piezoresistive detection, respectively (Fig. 4(c)). The gyrator in Fig. 4(b) relates the variables in the magnetic and the electrical domain. The gyrator equations are given by Ampères circuit law and Faraday's law of electromagnetic induction. Finally, the static or true electrical contributions are represented by the capacitor C_o, the inductor L_o and the resistor R_o.

Table 2 presents approximate expressions of the circuit elements of the networks in

Table 2
Expressions for the components of the equivalent circuit diagrams (Γ_1, C_o, L_o, R_o, K_1^*) in Fig. 4 evaluated for wide ($b > 5h$) cantilever beam transducers as shown in Fig. 1. The meaning of the symbols is explained in Appendix I. Uniform coverage of the beam by the "electrodes" is assumed and further, Poisson ratios of all materials are assumed to be the same.

Transducer mechanism	Γ_1	$K_1^*/K_1\ (=\omega_*^2/\omega_1^2)$	Static component
Electrostatic ($w_o << d$, $V_P << V_{PI}$)	$\dfrac{\varepsilon_0 b l V_P}{d^2}\chi_1$	$1-0.28\left(\dfrac{V_P}{V_{PI}}\right)^2$	$C_o = \dfrac{\varepsilon_0 b l}{d}$
Electrodynamic	$B_0 l \chi_1$	1	$L_o = L_s$
Dielectric ($E_f = E_s$, $\eta = \dfrac{\varepsilon_f V_f^2}{h_f^2 E_f/(1-\nu^2)}$)	$\dfrac{\nu\varepsilon_f V_f h_s b}{2(1-\nu)(1-\eta)h_f}\phi_1'(l)$	$1-\dfrac{3\nu^2(1+\nu)}{(1-\nu)^3}\dfrac{\eta}{1-\eta}\dfrac{h_f h_s^2}{(h_f+h_s)^3}$	$C_o = \dfrac{\varepsilon_f b l}{h_f}\left(1-\dfrac{2\nu^2}{(1-\nu)^3}\dfrac{\eta}{1-\eta}\right)$
Piezoelectric ($1/s_{11}^D = E_s$)	$\dfrac{d_{31} h_s b}{2 s_{11}^E (1-\nu)}\phi_1'(l)$	$1-3k_{31}^2\dfrac{(1+\nu)}{(1-\nu)}\dfrac{h_p h_s^2}{(h_p+h_s)^3}$	$C_o = \dfrac{\varepsilon_{33}^T b l}{h_p}\left(1-\dfrac{2}{1-\nu}k_{31}^2\right)$
Electromagnetic ($w_o << d$, $I_P << I_{PI}$)	$N^2\dfrac{\mu_0 b l I_P}{d^2}\chi_1$	$1-0.28\left(\dfrac{I_P}{I_{PI}}\right)^2$	$L_o = N^2\dfrac{\mu_0 b l}{d}$
Electrothermal excitation ($\omega << \omega_t^{(57)}$ and $h_R << h$)	$\dfrac{Eh^3\alpha\rho_o I_o}{12\lambda b h_R}\phi_1'(l)$	1	$R_o = \dfrac{\rho_o l}{h_R b}$
Piezoresistive detection ($h_R << h$)	$\dfrac{G\rho_o h I_o}{2 b h_R}\phi_1'(l)$	1	$R_o = \dfrac{\rho_o l}{h_R b}$

Fig. 4, evaluated for cantilever transducers and restricted to the most important physical mechanisms. It is assumed that the cantilevers are uniformly excited by the transducer elements. The latter implies, for instance, that the electrode in the case of electrostatic drive uniformly covers the beam surface, and similarly, the resistor for the electrothermal transducer consists of a thin sheet uniformly covering the beam surface. Note the bias dependence of the generalized stiffness K_1^*, and thus of the corresponding resonant frequency ω_*, for a number of transducer mechanisms.[53] An applied bias (including the internal bias of the piezoelectric case which is represented by the piezoelectric coefficient d_{31}) always leads to a lowering of the resonant frequency compared to the resonant frequency ω_1 of the system without electromechanical coupling.[32,53]

It is pointed out that each of the equivalents circuits of Fig. 4 represents the appropriate transducer element together with the spring stiffness of the vibrating member. The equivalent network of the *entire* resonator or better system is obtained by adding the appropriate loads and elements.[86,87] For instance, consider a one-port resonator without any parasitic electrical and mechanical loads. Its equivalent network is derived from any of the basic circuits of Fig. 4 by adding to the mechanical port a series connection of the (generalized) mass and damper as shown in Fig. 5(a). For an electrostatically driven

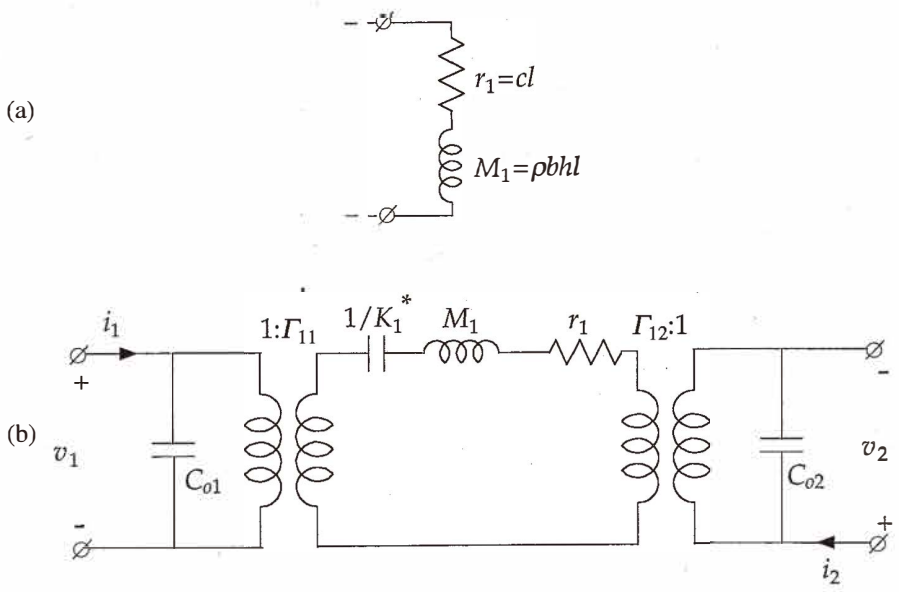

Fig. 5. (a) Network representing a mechanical load consisting of the generalized mass $M_1 = \rho bhl$ and the generalized damping parameter $r_1 = cl$. Connecting this network to the mechanical port in any of the equivalent networks in Fig. 4 results in the overall equivalent network of a one-port resonator (excluding any electric or mechanical parasitic loads). (b) Equivalent network of an electrostatically, piezoelectrically or dielectrically driven *two-port* resonator as obtained from the basic building blocks of Figs. 4(a) and 5(a). The second subscript in the transduction factors Γ_{11} and Γ_{12}, and the static capacitances C_{o1} and C_{o2} designates the port #.

resonator, a parasitic parallel capacitor C_p (as in Fig. 3(b)) is simply included by placing it parallel to C_o in Fig. 4(a) (see also refs. 86 and 87). In the case of an electrostatically (or piezoelectrically) driven *two-port* resonator, the network of Fig. 4(a) is extended to include not only the mass and damping of the vibrating member, but also the second transducer element, resulting in the network of Fig. 5(b). It is left to the reader to construct the equivalent networks based on the models of Fig. 4 for other forms of loading and different resonator configurations.

6. Conclusions

In this paper, three elementary design considerations that are essential for successful resonator application have been discussed. First of all, the *physical transduction mechanisms* that can be used for excitation and detection of the vibrational motion of silicon-based resonators have been described and classified according to power consumption, complexity and IC compatibility of technology, and influence on the resonator characteristics. A single arrangement of the mechanisms in order of performance cannot be given, and the choice of a specific mechanism is part of a decision process summarizing the pro's and con's with respect to the application, desired performance and resources available. Secondly, a distinction can be made between one- and two-port resonators, depending on the *number of transducer elements* used for a single resonator. The choice of the electrical configuration is reflected in the layout, in the number of interconnecting wires, and in the susceptibility to external electrical (parasitic) loads. Thirdly, the *exact position of the transducer element* varies from direct placement on the vibrating member, via placement on the base of the vibrating member, to placement external to the vibrating member. It has been elucidated in this paper that in deciding on the element position, a compromise should be sought between sufficient excitation/detection and a minimal effect of the element on the resonator characteristics.

Equivalent circuit representations that are useful for improving the understanding, design and analysis of the resonator have been presented. For instance, they assist in the design stage of interface electronics (*e.g.*, a feedback oscillator), and can be used to study the degrading effect of external electrical and mechanical loads. Furthermore, through the equivalent circuits the resonator can easily be embedded in a larger circuit and analyzed using appropriate circuit simulation software.

Appendix I: List of Symbols for Table 2

b cantilever width (see Fig. 1(i)) [m]
B_o applied bias magnetic induction (see Fig. 1(b)) [T]
d zero-voltage gap spacing (see Figs. 1(a) and 1(e)) [m]
d_{31} piezoelectric constant [C/N]
E Young's modulus of the beam material [Pa]
E_f Young's modulus of the dielectric film (in Fig. 1(c)) [Pa]

E_s Young's modulus of the carrier beam (in Fig. 1(c)) [Pa]
G longitudinal gauge factor of the resistor material [–]
h total cantilever thickness (see Figs. 1(i) and 1(c)) [m]
h_f thickness of the dielectric layer (see Fig. 1(c)) [m]
h_p thickness of the piezoelectric layer (see Fig. 1(c)) [m]
h_R thickness of the sheet resistor [m]
h_s carrier beam thickness (see Fig. 1(c)) [m]
I_P d.c. bias current of the electromagnetic transducer [A]
I_{PI} pull-in current of the electromagnetic transducer [A]
k_{31} material coupling factor, $k_{31}^2 = d_{31}^2 / \left(\varepsilon_{33}^T s_{11}^E \right)$ [41,42] [–]
l cantilever length (see Fig. 1(i)) [m]
L_s self-inductance of the current loop for the electrodynamic transducer [H]
N number of turns of the driving coil for the electromagnetic and magnetostrictive transducers [–]
s_{11}^D $(= s_{11}^E \left(1 - k_{31}^2\right))$ compliance of the piezoelectric layer at constant electric displacement[41,42] [Pa^{-1}]
s_{11}^E compliance of the piezoelectric layer at constant field[41,42] [Pa^{-1}]
V_f applied d.c. bias voltage across the dielectric layer [V]
V_P externally applied d.c. bias voltage[37] of the electrostatic transducer [V]
V_{PI} pull-in voltage[37] of the electrostatic transducer [V]
w_o static deflection due to the applied bias [m]
α thermal expansion coefficient of the beam material [K^{-1}]
χ_1 mode shape factor, defined by, $\chi_1 \equiv \frac{1}{l} \int_0^l \phi_1(x) \mathrm{d}x$ [–]
ε_0 permittivity of free space [F/m]
ε_{33}^T permittivity of the piezoelectric layer at constant stress[41,42] [F/m]
ε_f permittivity of the dielectric film [F/m]
λ thermal conductivity of the beam material [$Wm^{-1}K^{-1}$]
μ_0 permeability of free space [H/m]
ν Poisson's ratio [–]
ω radial frequency [$rad.s^{-1}$]
ω_1 fundamental resonant frequency in the absence of electromechanical coupling [$rad.s^{-1}$]
ω_* appropriate fundamental resonant frequency in the presence of electromechanical coupling [$rad.s^{-1}$]
ω_t characteristic frequency defininining the transition from thermally thin to thermally thick beams, $\omega_t = 12\lambda / \rho c h^2$[57] [$rad.s^{-1}$], where c is the heat capacity of the beam material [$Jkg^{-1}K^{-1}$]
ρ specific mass of the beam material [kgm^{-3}]
ρ_o specific resistance at the bias point defined by a bias stress and a bias temperature [Ωm]

References

1 J. C. Greenwood: Silicon Transducer (Patent specification 1588669, London, 1978).
2 J. G. Smits, H. A. C. Tilmans, K. Hoen, H. Mulder, J. van Vuuren and G. Boom: Sensors and Actuators **4** (1983) 565.

3 J. C. Greenwood: J. Phys. E: Sci. Instrum. **17** (1984) 650.
4 J. G. Smits, H. A. C. Tilmans and T. S. J. Lammerink: Proc. 3rd Int. Conf. Solid-State Sensors and Actuators (Transducers '85), Philadelphia, PA, U.S.A., June 11–14 (1985) p. 93.
5 T. S. J. Lammerink and W. Wlodarski: Proc. Int. Conf. Solid-State Sensors and Actuators (Transducers '85), Philadelphia, PA, U.S.A., June 11–14 (1985) p. 97.
6 K. Ikeda, H. Kuwayama, T. Kobayashi, T. Watanabe, T. Nishikawa and T. Yoshida: Proc. of the 7th Sensor Symp., Tokyo, Japan, May 30–31 (1988) p. 55.
7 D. W. Satchell and J. C. Greenwood: Sensors and Actuators **17** (1989) 241.
8 S. Bouwstra, P. Kemna and R. Legtenberg: Sensors and Actuators **20** (1989) 213.
9 F. R. Blom, S. Bouwstra, J. H. J. Fluitman and M. Elwenspoek: Sensors and Actuators **17** (1989) 513.
10 J. J. Sniegowski, H. Guckel and T. R. Christenson: Tech. Dig. IEEE Solid-State Sensor and Actuator Workshop, Hilton Head Island, SC, U.S.A., June 4–7 (1990) p. 9.
11 R. A, Buser, N. F. deRooij and L. Schultheis: Sensors and Actuators A **25–27** (1991) 717.
12 K. Petersen, F. Pourahmadi, J. Brown, P. Parsons, M. Skinner and J. Tudor: Proc. 6th Int. Conf. Solid-State Sensors and Actuators (Transducers '91), San Francisco, U.S.A., June 24–27 (1991) p. 664.
13 H. A. C. Tilmans, M. Elwenspoek and J. H. J. Fluitman: Sensors and Actuators A **30** (1992) 35.
14 A. D. Nikolich and S. D. Senturia: Tech. Digest, IEEE Solid-State Sensors Workshop, Hilton Head Island, SC, U.S.A., June 22–25 (1992) p. 157.
15 H. A. C. Tilmans and M. Elwenspoek: J. Micromechanics and Microengineering **3** (1993) 193.
16 H. A. C. Tilmans, R. Legtenberg, H. Schurer, D. J. IJntema, M. Elwenspoek and J. H. J. Fluitman: IEEE Trans. Ultrasonics, Ferroelectrics and Frequency Control **41** (1994) 4.
17 Th. Fabula, H.-J. Wagner, B. Schmidt and S. Büttgenbach: Sensors and Actuators A **41–42** (1994) 375.
18 D. W. Burns, J. D. Zook, R. D. Horning, W. R. Herb and H. Guckel: Tech. Dig. Solid-State Sensor and Actuator Workshop, Hilton Head Island, SC, U.S.A., June 13–16 (1994) p. 221.
19 D. B. Hicks, S. -C. Chang, M. W. Putty and D. S. Eddy: Tech. Dig. Solid-State Sensor and Actuator Workshop, Hilton Head Island, SC, U.S.A., June 13–16 (1994) p. 225.
20 E. Stemme and G. Stemme: IEEE Trans. Electron Devices **37** (1990) 648.
21 R. T. Howe and R. S. Muller: IEEE Trans. Electron Devices **ED-33** (1986) 499.
22 W. Benecke, L. Csepregi, A. Heuberger, K. Kühl and H. Seidel: Proc. 3rd Int. Conf. Solid-State Sensors and Actuators (Transducers '85), Philadelphia, PA, U.S.A., June 11–14 (1985) p. 105.
23 O. Brand, H. Baltes and U. Baldenweg: Proc. IEEE Micro Electro Mechanical Systems (MEMS'94), Oiso, Japan, Jan. 25–28 (1994) p. 33.
24 H. C. Nathanson, W. E. Newell, R. A. Wickstrom and J. R. Davis, Jr.: IEEE Trans. Electron Devices **ED-14** (1967) 117.
25 M. F. Hribsek and R. W. Newcomb: IEEE Trans. Circuits and Systems **CAS-25(4)** (1978) 215.
26 L. Lin, C. T. - C. Nguyen, R. T. Howe and A. P. Pisano: Proc. IEEE Micro Electro Mechanical Systems (MEMS'92), Travemünde, Germany, Feb. 4–7 (1992) p. 226.
27 A. P. Lee and A. P. Pisano: J. of Microelectromechanical Systems **1** (1992) 70.
28 C. H. Hsu and R. S. Muller: Proc. 6th Int. Conf. Solid-State Sensors and Actuators (Transducers '91), San Francisco, U.S.A., June 24–27 (1991) p. 659.
29 C. T. - C. Nguyen and R. T. Howe: Proc. 7th Int. Conf. Solid-State Sensors and Actuators (Transducers '93), Yokohama, Japan, June 7–10 (1993) p. 1040.
30 M. Elwenspoek: Journal A **32** (1991) 15.
31 G. Stemme: J. Micromechanics and Microengineering 1 (1991) 113.
32 A. Prak, T. S. J. Lammerink and J. H. J. Fluitman: Sensors and Materials **5** (1993) 143.

33 R. Buser: Resonant sensors, in Sensors - A comprehensive survey, W. Göpel, J. Hess and J. N. Zemel (series eds.), vol. 7: Mechanical sensors, H. H. Bau, B. Kloeck and N. F. de Rooij (vol. eds.) (VCH, P.O. Box 101161, D-6940 Weinheim, Germany, 1994) p. 205.
34 M. W. Putty, S. C. Chang, R. T. Howe, A. L. Robinson and K. D. Wise: Proc. IEEE Micro Electro Mechanical Systems (MEMS'89), Salt Lake City, Utah, U.S.A., Feb. 20–22 (1989) p. 60.
35 R. A. Buser and N. F. de Rooij: Proc. IEEE Micro Electro Mechanical Systems (MEMS'90), Napa Valley, California, U.S.A., Feb. 11–14 (1990) p. 132.
36 C. Linder, E. Zimmerman and N. F. de Rooij: Sensors and Actuators A **25–27** (1991) 591.
37 H. A. C. Tilmans and R. Legtenberg: Sensors and Actuators A **45** (1994) 67.
38 C. Cabuz, S. Shoji, K. Fukatsu, E. Cabuz, K. Minami and M. Esashi: Sensors and Actuators A **43** (1994) 92.
39 R. A. Buser and N. F. de Rooij: Proc. IEEE Micro Electro Mechanical Systems (MEMS'89), Salt Lake City, Utah, U.S.A. Feb. (1989) p. 126.
40 C. J. van Mullem, H. A. C. Tilmans, A. J. Mouthaan and J. H. J. Fluitman: Sensors and Actuators A **31** (1992) 168.
41 D. A. Berlincourt, D. R. Curren and H. J. Jaffe: Piezoelectric and Piezomagnetic Materials and Their Function in Transducers, Physical Acoustics, vol. IA, ed. W. P. Mason (Academic Press, New York, 1964) p. 169.
42 T. Ikeda: Fundamentals of Piezoelectricity (Oxford University Press, New York, 1989).
43 T. Shiosaka and A. Kawabata: Appl. Phys. Lett. **25** (1974) 10.
44 D. L. Polla and R. S. Muller: Tech. Digest IEEE Solid-State Sensors Workshop, Hilton Head Island, SC, U.S.A., June 6–9 (1986).
45 F. R. Blom, D. J. Yntema, F. C. M. van de Pol, M. Elwenspoek, J. H. J. Fluitman and Th. J. A. Popma: Sensors and Actuators A **21–23** (1990) 226.
46 M. Okuyama and Y. Hamakawa: Sensors and Materials **1** (1988) 013.
47 D. L. Polla, T. Tamagawa, C. Ye. P. Schiller, L. Pham and C.-Y. Tu: Proc. SPIE **1694** (1992) p. 173.
48 S. Bouwstra, F. R. Blom, T. S. J. Lammerink, H. Untema, P. Schrap, J. H. J. Fluitman and M. Elwenspoek: Sensors and Actuators **17** (1989) 219.
49 E. Quandt, B, Gerlach, T. Gerst, K. Seemann: Proc. Actuator 94, Bremen, Germany, June 15–17 (1994) p. 229.
50 T. Honda, K. I. Arai and M. Yamaguchi: Proc. IEEE Micro Electro Mechanical Systems (MEMS'94), Oiso, Japan, Jan. 25–28 (1994) p. 51.
51 G. Flik, M. Schnell, F. Schatz and M. Hirscher: Proc. Actuator 94, Bremen, Germany, June 15–17 (1994) p. 232.
52 H. H. Woodson and J. R. Melcher: Electromechanical Dynamics, Parts I, II and III (Wiley, New York, 1968).
53 H. A. C. Tilmans: Micromechanical sensors using encapsulated built-in resonant strain gauges (Ph.D. dissertation, Faculty of Electrical Eng., Univ. of Twente, Jan. 1993) Ch. 3.
54 R. J. Wilfinger, P. H. Bardell and D. S. Chhabra: IBM J. Res. Develop. **12** (1968) 113.
55 M. B. Othman and A. Brunnschweiler: Electron. Lett. **23** (1987) 728.
56 D. Moser, O. Brand and H. Baltes: Proc. 6th Int. Conf. Solid-State Sensors and Actuators (Transducers '91), San Francisco, U.S.A., June 24–27 (1991) p. 547.
57 T. S. J. Lammerink, M. Elwenspoek and J. H. J. Fluitman: Sensors and Materials **3** (1992) 217.
58 M.-A. Grétillat, C. Linder and N. F. de Rooij: Sensors and Actuators A **43** (1994) 351.
59 Chr. Burrer and J. Esteve: Sensors and Actuators A **41–42** (1994) 680.
60 M. Hoffmann, H. Bezzaoui and E. Voges: Sensors and Actuators A **44** (1994) 71.
61 E. Dieulesaint, D. Royer and C. Bonnefoy: IEEE Proc. 1981 Ultrasonics Symp. (1981) p. 802.

62 S. Venkatesh and B. Culshaw: Electron. Lett. **21** (1985) 315.
63 W. Benecke, A. Heuberger, W. Riethmüller, U. Schnakenberg, H. Wölfelschneider, R. Kist, G. Knoll, S. Ramakrishnan and H. Höfflin: Proc. Int. Conf. Solid-State Sensors and Actuators (Transducers '87), Tokyo, Japan (1987) p. 838.
64 K. E. B. Thornton, D. Uttamchandani and B. Culshaw: Sensors and Actuators A **24** (1990) 15.
65 D. Walsh and B. Culshaw: Sensors and Actuators A **25–27** (1991) 711.
66 R. M. A. Fatah: Sensors and Actuators A **33** (1992) 229.
67 A. V. Churenkov: Sensors and Actuators A **39** (1993) 141.
68 H. Guckel, M. Nesnidal, J. D. Zook and D. W. Burns: Proc. 7th Int. Conf. Solid-State Sensors and Actuators (Transducers '93), Yokohama, Japan, June 7–10 (1993) p. 686.
69 T. S. J. Lammerink and S. J. Gerritsen: Proc. SPIE **798** (1987) p. 67.
70 J. A. Dziuban, A. Gorecka-Drzazga and U. Lipowicz: Sensors and Actuators A **32** (1992) 628.
71 D. Garthe: Sensors and Actuators A **37–38** (1993) 484.
72 M. J. Tudor, M. V. Andres, K. W. H. Foulds and J. M. Naden: IEE Proceedings **135** (1988) 364.
73 M. V. Andres, K. W. H. Foulds and M. J. Tudor: Sensors and Actuators **15** (1988) 417.
74 G. Higelin and V. Lange: Proc. Micro System Technologies '94, Berlin, Oct. 19–21 (1994) p. 87.
75 D. Stöckel: Proc. Actuator 92, Bremen, Germany, June 24–26 (1992) p. 79.
76 M. Hashimoto, C. Cabuz, K. Minami and M. Esashi: Proc. Micro System Technologies '94, Berlin, Oct. 19–21 (1994) p. 763.
77 T. S. J. Lammerink, M. Elwenspoek, R. H. van Ouwerkerk, S. Bouwstra and J. H. J. Fluitman: Sensors and Actuators A **21–23** (1990) 352.
78 B. Geijselaers and H. Tijdeman: Sensors and Actuators A **29** (1991) 37.
79 L. M. Zhang, D. Uttamchandani, B. Culshaw and P. Dobson: Meas. Sci. Technol. **1** (1990) 1343.
80 J. Elders, H. A. C. Tilmans, S. Bouwstra and M. Elwenspoek: Materials Research Society Symposium Proceedings, Thin Films: Stresses and Mechanical Properties IV, MRS Spring Meeting 1993, San Francisco, USA **308** (1993) p.171.
81 S. P. Timoshenko, D. H. Young and W. Weaver: Vibration Problems in Engineering (John Wiley & Sons, New York, 1974) 4th ed., Chap. 5.
82 S. Bouwstra, J. van Rooijen, H. A. C. Tilmans, A. Selvakumar and K. Najafi: Sensors and Actuators A **37–38** (1993) 38.
83 R. A. Brennen, A. P. Pisano and W. C. Tang: Proc. IEEE Micro Electro Mechanical Systems (MEMS'90), Napa Valley, California, USA, Feb. 11–14 (1990) p. 9.
84 H. A. C. Tilmans, D. J. IJntema and J. H. J. Fluitman: Proc. 6th Int. Conf. Solid-State Sensors and Actuators (Transducers '91), San Francisco, CA, U.S.A., June (1991) p. 533.
85 W. H. Hayt, Jr. and J. E. Kemmerly: Engineering Circuit Analysis (McGraw-Hill, New York, 1978) Chap. 16.
86 H. A. C. Tilmans: J. of Micromechanics and Microengineering **6** (1996) 157.
87 H. A. C. Tilmans: Equivalent circuit representation of electromechanical transducers, Part II: Distributed-parameter systems, in preparation (1996).
88 C. J. van Mullem, F. W. A. van Dam, J. H. J. Fluitman and H. Wallinga: Proc. 7th Int. Conf. Solid-State Sensors and Actuators (Transducers '93), Yokohama, Japan, June 7–10 (1993) p. 787.
89 L. Meirovitch: Elements of Vibration Analysis (McGraw-Hill, New York, 1975).

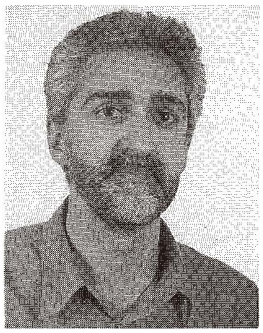

Harrie Tilmans received his M.Sc. in Electrical Engineering from the University of Twente, Enschede, The Netherlands, in May 1984, and his Ph.D. in Electrical Engineering from the same university in January 1993.

In June 1984 he became a research associate in the micromechanics group of the University of Twente. In April 1985 he joined the faculty of Electrical and Computer Engineering of Boston University, Boston, MA, U.S.A., as a visiting instructor. In August 1986 he became a research assistant at the Wisconsin Center for Applied Microelectronics at the University of Wisconsin-Madison, U.S.A. After a period of two years, he returned to The Netherlands where he joined the MESA Research Institute of the University of Twente as a research associate to work on "micromechanical sensors using encapsulated built-in resonant strain gauges", which became the subject of his dissertation. From August 1989 to January 1990 he was on leave from the university to join the Sensors group of the Controls Research Department of Johnson Controls Inc., Milwaukee, WI, U.S.A., where he worked on a low-range differential resonant pressure sensor. From September 1, 1992 to August 1, 1993 he accepted a postdoctorate position within the micromechanics group of the MESA Research Institute, which was offered by F.O.M. (Foundation for Fundamental Research on Matter, The Netherlands). From November 1993 to September 1995 he was employed as a research associate by the Catholic University of Leuven, Belgium where he continued his work on micromechanical sensors, actuators and systems. Since October 1, 1995 he has been employed by CP Clare Corporation (Tongeren, Belgium), a worldwide manufacturer of relays and switches, as an R&D project manager.

Dr. Tilmans is a member of the IEEE's Magnetics Society and the IEEE Ultrasonics, Ferroelectrics and Frequency Control Society.

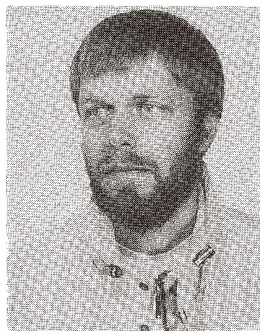

Siebe Bouwstra received his M.Sc. in Mechanical Engineering from the University of Twente, Enschede, The Netherlands, in March 1984. He has been active in micromechanics ever since, spending two years in an industrial project for Oce van der Grinten b.v. (Venlo, The Netherlands), and four years in a government-funded project in collaboration with ASM International b.v. (Bilthoven, The Netherlands). He received his Ph.D. in Applied Physics from the University of Twente in March 1990, based on his dessertation "Resonating Microbridge Mass Flow Sensor". He was Fellow of the Royal Dutch Academy of Sciences, during which he initiated a collaboration with the Center for Integrated Sensors and Circuits of the University of Michigan, U.S.A. In November 1992 he was appointed Associate Professor at the brand new national institute Mikroelektronik Centret at the Technical University of Denmark, where he is responsible for developing a micromechanics programme.